

Effect of Bias in Contrast Agent Concentration Measurement on Estimated Pharmacokinetic Parameters in Brain Dynamic Contrast-Enhanced Magnetic Resonance Imaging Studies

Azimeh NV Dehkordi^{1*}

1. Department of Physics, Najafabad Branch, Islamic Azad University, Najafabad, Iran

ARTICLE INFO

Article type:
Original Article

Article history:

Received: Jun 26, 2019

Accepted: Aug12, 2019

Keywords:

Dynamic Contrast-Enhanced Magnetic Resonance Imaging Kinetic Analysis Contrast Concentration Bias MPE of PK Parameters

ABSTRACT

Introduction: Pharmacokinetic (PK) modeling of dynamic contrast-enhanced magnetic resonance imaging (DCE-MRI) is widely applied in tumor diagnosis and treatment evaluation. Precision analysis of the estimated PK parameters is essential when they are used as a measure for therapy evaluation or treatment planning. In this study, the accuracy of PK parameters in brain DCE-MRI studies was quantified in relation to two major sources of error (including pre-contrast longitudinal-relaxation time, $T_{1,0}$ and flip angle, α).

Material and Methods: 3470 dynamic contrast-enhanced-curves were simulated using a wide variation of the PK parameters. The bias of contrast concentration due to the systematic biases in α and $T_{1,0}$ was calculated and added to both contrast concentration and AIF profiles. Thereafter, the PK parameters were estimated for each simulated curve in the presence of different percentages of relative biases in α and $T_{1,0}$. The mean percentage error (MPE) of PK parameters was then calculated for all simulated curves.

Results: The results indicated that plasma volume (v_p) was the most sensitive parameter to bias of contrast concentration, which may overestimate up to 700% in 10% coincidence relative bias in α and $T_{1,0}$. The lowest MPE was related to the backward transfer constant (k_{ep}), which was ~2%-15% in 10% coincidence relative bias in each α and $T_{1,0}$.

Conclusion: Utilization of a nested model selection technique, along with an accurate estimator, such as maximum-likelihood estimation, created a unique approach for investigating the effect of the bias in the concentration measurement to the estimated PK parameters without the addition of any extra biases to the parameters during the estimation.

► Please cite this article as:

Dehkordi A. Effect of Bias in Contrast Agent Concentration Measurement on Estimated Pharmacokinetic Parameters in Brain Dynamic Contrast-Enhanced Magnetic Resonance Imaging Studies. Iran J Med Phys 2020; 17:142-152. 10.22038/ijmp.2019.41400.1598.

Introduction

Pharmacokinetic (PK) modeling of dynamic contrast-enhanced magnetic resonance imaging (DCE-MRI) is widely applied in tumor diagnosis and treatment evaluation [1-3]. Precision analysis of the estimated PK parameters is considered essential to DCE-MRI studies, especially when PK parameters are used as a measure for therapy evaluation or treatment planning [1, 4]. There are different sources of bias in contrast agent (CA) concentration that can contribute to bias in the estimates of PK parameters. The major sources of biases in the measured CA concentration using spoiled gradient-echo (SPGR) pulse sequence include biases in intrinsic tissue properties (pre-contrast longitudinal and transverse relaxation time, $T_{1,0}$, $T_{2,0}^*$, and longitudinal and transverse contrast relaxivities, r_1 , r_2) and imaging sequence parameters, such as flip angle, α , Echo Time, T_E , and Repetition Time, T_R [5-7]. Bias in CA concentration significantly incorporates the pharmacokinetic models and consequently contribute to estimated PK parameters [7, 8]. Moreover, the accurate quantification of the

arterial input function (AIF) is also a critical step in the estimation of PK parameters and exerts a significant effect on this bias [9, 10]. The different systematic biases in CA concentration obtained in T_1 -weighted DCE-MRI has been investigated by a few researchers [7, 8, 11-13] and biases in measured concentration were reported to be highly dependent on the sequence parameters. A recently published literature by Schabel and Parker [11] derived a closed-form expression for concentration measurement bias since it depends on bias of flip angle (α), pre-contrast longitudinal and transverse relaxation time ($T_{1,0}$ and $T_{2,0}^*$, respectively), as well as longitudinal and transverse contrast relaxivities (r_1 and r_2 , respectively). The reported equations signified that the misspecification in $T_{1,0}$ and α produce dominant biases in CA concentration over the most range of the assured concentration. However, a few studies have investigated the precision of the estimated PK parameters [7, 8, 11, 12], and to the best of our knowledge, there is no study on the direct

quantification of such uncertainties in the accuracy of the estimated PK parameters.

Selection of a correct model to describe the tissue concentration, as well as a minimum variance unbiased estimator to estimate the PK parameters is crucial in the pharmacokinetic analysis of DCE-MRI. Naeyer et al. [12] previously reported that the uncertainty of PK parameters can be reduced up to 30% when estimated by maximum likelihood estimation (MLE) technique, instead of least square error technique.

Accordingly, the extended Toft-model combined with model selection (MS) technique [5, 14] and MLE [15], were utilized in the current study to investigate the propagation of two major sources of systematic uncertainties in the CA concentration to the estimated PK parameters in brain DCE-MRI studies.

Materials and Methods

Simulation of Contrast Agent Concentration Profiles

Extended Toft-Model is the most popular pharmacokinetic model widely used in the pharmacokinetic analysis of DCE-MRI studies. In this regard, a set of CA concentration profiles was simulated using the extended Tofts equation with a wide variation of PK parameters (Table 1) to evaluate the sensitivity of CA concentration profiles to the biases in pre-contrast T_1 ($T_{1,0}$), and flip angle. According to MS concept [5, 14], three physiologically nested models extracted from extended Tofts-equation were constructed: Model 1 for tissues with no vascular leakage (normal tissue) (Equation 1), Model 2 for tissues with leakage without efflux (Equation 2), and Model 3 for tissues with leakage and bidirectional exchange (influx and efflux) (Equation 3) [5]. A population-averaged AIF was used to simulate the CA concentration profiles.

$$\text{Model 1: } C(t) = v_p \cdot \text{AIF}(t) \tag{1}$$

$$\text{Model 2: } C(t) = K^{\text{trans}} \int_0^t \text{AIF}(\tau) \cdot d\tau + v_p \cdot \text{AIF}(t) \tag{2}$$

$$\text{Model 3: } C(t) = K^{\text{trans}} \int_0^t \text{AIF}(\tau) \cdot e^{-k_{\text{ep}}(t-\tau)} d\tau + v_p \cdot \text{AIF}(t) \tag{3}$$

In Equations 1, 2, and 3, $C(t)$ denotes the tissue CA concentration profiles. The v_p is blood plasma volume, K^{trans} and k_{ep} are forward and backward transverse constants, and AIF is plasma CA concentration. Using Equation 1, 10 CA concentration profiles were simulated and considered as the Model 1 profiles by varying v_p from 0.5% to 9.5%. Using Equations 2, 310 CA concentration profiles were simulated and considered as the Model 2 profiles by varying v_p from

0.5% to 9.5% and K^{trans} from 0.01 to 0.76 min^{-1} . Using Equation 3, the three PK parameters varied from 0.5% to 9.5%, 0.01 to 0.51 min^{-1} , and 0.035 to 0.735 min^{-1} for v_p , K^{trans} , and k_{ep} , respectively. Given the variation of the PK parameters mentioned above, 3150 CA concentration profiles were simulated and considered as the Model 3 profiles. The increments of the PK parameters in different models were 1% (v_p for all 3 models), 0.025 min^{-1} (K^{trans} for model 2 and 3) and 0.001 min^{-1} (k_{ep} for model 3) [16].

Calculation of Contrast Agent Concentration Bias

In DCE-MRI and SPGR imaging protocol, the signal intensity (S) is constructed in effect of the following parameters (Eq. 4) [11]:

$$S(T_1, T_2^*) = M_0 \frac{\sin \alpha (1 - e^{-T_R/T_1}) e^{-T_E/T_2^*}}{1 - e^{-T_R/T_1} \cos(\alpha)} \tag{4}$$

Where, α is flip angle, T_R is repetition time, T_E is echo time, M_0 is equilibrium magnetization, T_1 is longitudinal relaxation time, and T_2^* is transverse relaxation time. The relative enhancement value of the MR intensity signal after CA injection can be calculated using the following equation (Equation 5) [11]:

$$\mu = \frac{S(T_1, T_2^*) - S(T_{1,0}, T_{2,0}^*)}{S(T_{1,0}, T_{2,0}^*)} \tag{5}$$

Where, $T_{1,0}$ and $T_{2,0}^*$ denotes pre-contrast longitudinal and transverse relaxation times, respectively. An analytical formalism can be defined for CA concentration using the above equation and assuming a linear approximate relationship between contrast concentration and longitudinal relaxation rate ($R_{1,0} = 1/T_{1,0}$) [11, 17]:

$$C \approx \frac{1}{r_1} R_{1,0} \mu \tag{6}$$

The acquisition parameters for imaging, such as T_R and T_E can be adjusted in a reasonable accuracy. The tuned flip angle (α) during the imaging sequence may vary significantly from its nominal value, especially at a higher magnetic field strength. In addition, the precision of pre-contrast longitudinal time ($T_{1,0}$) measuring is limited during the imaging sequence due to environmental inhomogeneity, partial volume effect, and flow effects. Accordingly, it is mandatory to investigate the effect of misspecification in these two parameters (α and $T_{1,0}$) on the bias of the CA concentration measurement.

Table 1. Variation of Pharmacokinetic parameters for simulating Model 1, 2 and 3 profiles

	v_p	K^{trans}	k_{ep}
Model 1	0.5%-9.5%	-	-
Model 2	0.5% - 9.5%	0.01 to 0.76 min^{-1}	-
Model 3	0.5%-9.5%	0.01 to 0.51 min^{-1}	0.035 to 0.735 min^{-1}

Table 2. Intrinsic tissue properties for water, plasma and blood part of the brain in 3T

Tissue	r_1 (mmol ⁻¹ s ⁻¹)	r_2 (mmol ⁻¹ s ⁻¹)	$T_{1,0}$ (ms)	$T_{2,0}^*$ (ms)
Water	3.1	3.7	5000	3125
Plasma	3.7	5.2	2272	344
Blood	3.9	6.9	1900	320

The uncertainty associated with the measured CA concentration due to the systematic biases in flip angle (α) and pre-contrast longitudinal time ($T_{1,0}$) was calculated according to the previously published formalism of Schabel and Parker [11] with the following DCE-MRI parameters: filed strength of 3T, temporal resolution of 5.035 sec, and flip angle= 20°, $T_E/T_R \sim 0.84/5.8$ ms. The sensitivity of the CA concentration to the flip angle (α) can be calculated according to Equation 7 [11]:

$$\frac{\partial C}{\partial \alpha} = -\frac{\sin \alpha (E_1 - 1)(E_1 - E_{1,0})}{\beta (E_{1,0} \cos \alpha - 1)} \quad (7)$$

In Equation 7; E_1 , $E_{1,0}$ and β are introduced as the following expressions [11]:

$$E_{1,0} = \exp\left(-\frac{T_R}{T_{1,0}}\right) \quad (8)$$

$$E_1 = \exp(-T_R R_1) \quad (9)$$

$$\beta = r_1 T_R E_1 (\cos \alpha - 1) + r_2^* T_E (E_1 - 1)(E_1 \cos \alpha - 1) \quad (10)$$

Where, $R_1 (=1/T_1)$ is the longitudinal relaxation rate, and r_1 and r_2^* are longitudinal and transverse contrast relaxivities. The intrinsic tissue properties, ($T_{1,0}$, r_1 , and r_2^*), for different brain tissues (e.g., blood, plasma, and water) in filed strength of 3T were determined according to the literature [18, 19] as depicted in Table 2. The sensitivity of the CA concentration to the pre-contrast longitudinal time ($T_{1,0}$) was calculated using the following equations [8, 11]:

$$\frac{\partial C}{\partial T_{1,0}} = -\frac{T_R (\cos \alpha - 1)}{\beta (E_{1,0} - 1)(E_{1,0} \cos \alpha - 1)} \times \left(E_1 (E_{1,0} - 1)(E_{1,0} \cos \alpha - 1) \frac{\partial R_1}{\partial T_{1,0}} + \frac{E_{1,0} (E_1 - 1)(E_1 \cos \alpha - 1)}{T_{1,0}^2} \right) \quad (11)$$

A wide range of relative biases from -20% underestimate to +20% overestimate was considered for each flip angle and $T_{1,0}$, and the sensitivity of the CA concentration was assessed for this range of biases. The previous literature [20] indicated that $T_{1,0}$ is not significantly dependent on flip angle; therefore, these two parameters were investigated independently in the present study. An accurate assessment can be achieved if only all the major sources of error are taken into account in the evaluation. The bias in α and $T_{1,0}$ generate uncertainty in AIF signal since AIF profile is generally selected from the measured CA concentration. Therefore, the propagated AIF error was also considered in all steps of the evaluations and the calculated bias of CA concentration was added to both AIF and simulated CA concentrations profiles.

Precision Analysis of the Estimated Pharmacokinetic Parameters

To investigate the propagation of the bias in CA concentration to estimated PK parameters, the PK parameters were estimated for each simulated CA concentration profile in the presence of different percentage relative biases in flip angle and $T_{1,0}$. The calculated bias of concentration arises from the biases in flip angle and $T_{1,0}$ were added to all simulated profiles and AIF signal (Equations 12-15) [8, 11]:

$$\delta C_\alpha = \frac{\partial C}{\partial \alpha} \delta \alpha \quad \cdot \quad \delta AIF_\alpha = \frac{\partial AIF}{\partial \alpha} \delta \alpha \quad (12)$$

$$\delta C_{T_{1,0}} = \frac{\partial C}{\partial T_{1,0}} \delta T_{1,0} \quad \cdot \quad \delta AIF_{T_{1,0}} = \frac{\partial AIF}{\partial T_{1,0}} \delta T_{1,0} \quad (13)$$

$$C(t)' = C(t) + \delta C_\alpha + \delta C_{T_{1,0}} \quad (14)$$

$$AIF(t)' = AIF(t) + \delta AIF_\alpha + \delta AIF_{T_{1,0}} \quad (15)$$

In the next step, the PK parameters for the newly constructed signals were estimated. Thereafter, the mean percentage error (MPE) of the estimated PK parameters was calculated for all simulated CA concentrations profiles.

In this analysis, a recently developed algorithm based on MLE [15, 16] was utilized to estimate the PK parameters. The basic concept of MLE theory is to find the estimate of parameters (θ^{ML}) that maximizes the probability of the observed data [21]. In order to estimate the PK parameters, three nested models derived from the extended Tofts equation described in Eq 1-3 were considered and θ^{ML} was introduced as [v_p], [v_p , K^{trans}] and [v_p , K^{trans} and k_{ep}] for Model 1, 2 and 3 respectively.

Results

Figure 1 exhibits three examples of the simulated time-CA concentrations curves for Model 1 (blue curve), 2 (green curve), and 3 (red curve). To cover a reasonable variety of misspecifications, a wide range of relative bias (-20% to +20%) was considered for flip angle, the bias of CA concentration was then calculated and quantified for each relative bias. The calculated bias of CA concentration of Model 1, 2 and 3 versus different concentration values are depicted in figure 2-A to 2-C, 2-D to 2-F and 2-G to 2-I corresponding to water, plasma and blood part of the brain, respectively. As demonstrated in these plots, a positive bias in flip angle produces a negative bias in CA concentration for three models. The obtained results for three tissues indicate that propagated bias in CA concentration for Model 1, 2 and 3 are relatively in the same range; however, higher values of the CA concentrations are more sensitive to the bias of flip angle.

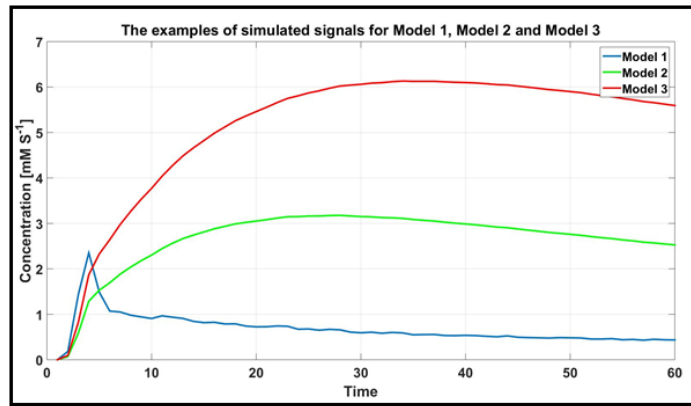


Figure 1. Three examples of the simulated signal profiles for Model 1 (blue curve), 2 (green curve), and 3 (red curve)

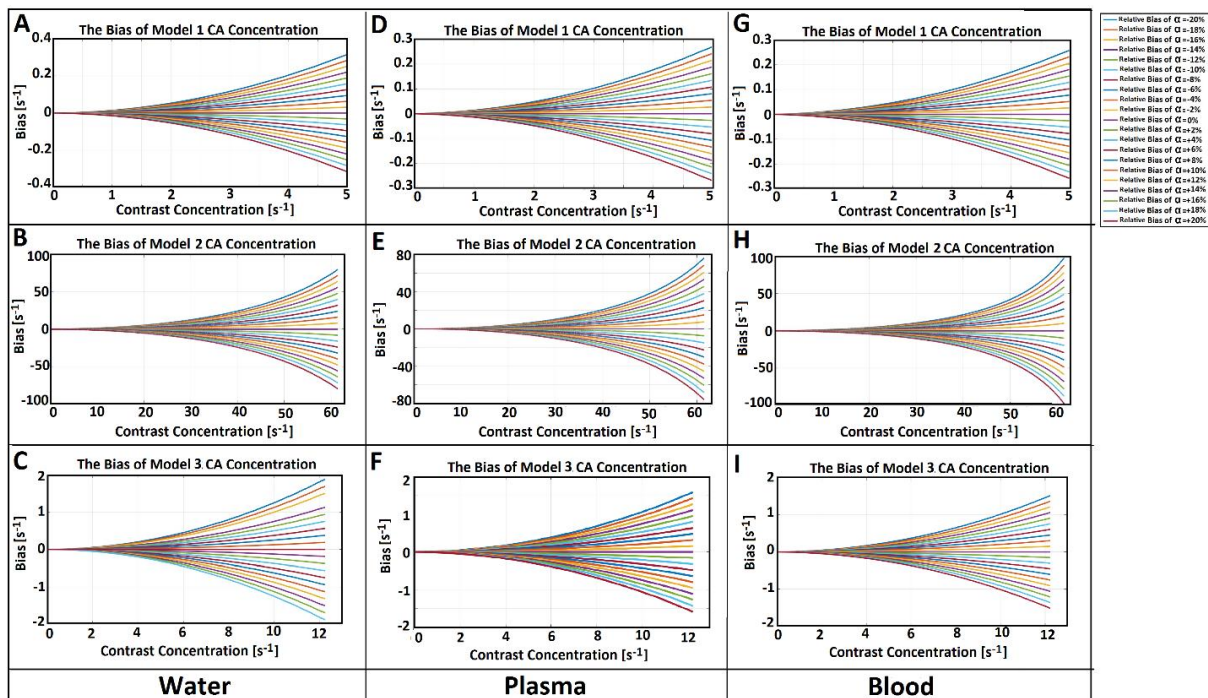


Figure 2. This figure displays the bias of the CA concentration of three simulated models, in comparison with different concentration values at different relative bias of flip angle (α). A) the bias of model 1 CA concentration in water part of the brain, B) the bias of model 2 CA concentration in water part of the brain, C) the bias of model 3 CA concentration in water part of the brain, D) the bias of model 1 CA concentration in plasma part of the brain, E) the bias of model 2 CA concentration in plasma part of the brain, F) the bias of model 3 CA concentration in plasma part of the brain, G) the bias of model 1 CA concentration in blood part of the brain, H) the bias of model 2 CA concentration in blood part of the brain, I) the bias of model 3 CA concentration in blood part of the brain.

Among the three models, the concentration profiles of Model 2 include higher CA concentration values; therefore, the highest calculated bias in CA concentration can be found in the second row of the figure (e.g., 20% overestimation in flip angle may induce a bias of $\sim 87 \text{ s}^{-1}$ in measured concentration with a value about 60 s^{-1}).

Figure 3 has three sub-plots that depict the mean relative bias percentage of CA concentration for three different brain tissues (i.e., water, plasma, and blood), compared to different relative biases of flip angle. As it can be observed, misspecification in flip angle is more affected on Model 2 CA concentration ($\sim \pm 22\%$ to

$\pm 28\%$), as compared to Model 1 ($\sim \pm 1.2\%$) or Model 3 ($\sim \pm 4.2\%$ to $\sim \pm 6\%$) in all studied brain tissues. Moreover, the measured concentration in water tissue is demonstrated to be more affected, in comparison to plasma and blood tissues, especially for Model 2 and 3.

Figure 4-A to 4-I depicts how the CA concentration values for three brain tissues are biased by the $T_{1,0}$ variations. The contribution from $T_{1,0}$ variation is plotted for water plasma, and blood tissues in the first, second, and third column, respectively. In low concentration values, the propagated bias in measured concentration is almost a linear function of concentration values.

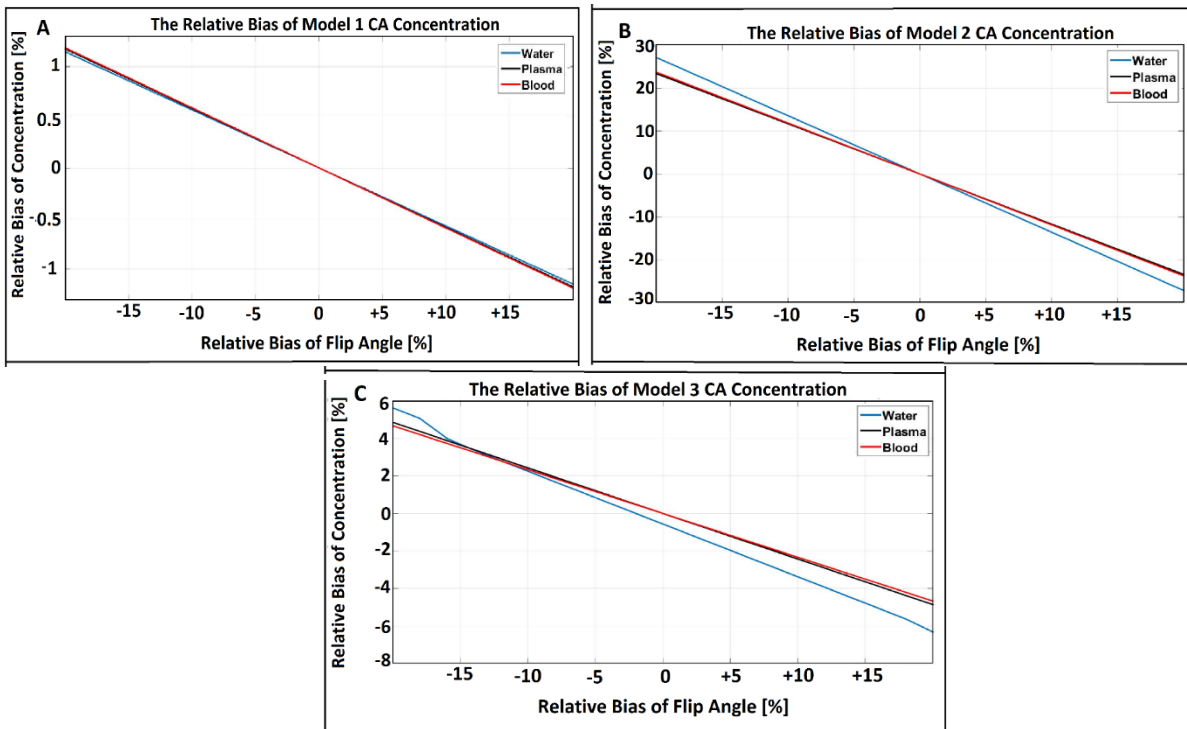


Figure 3. Mean relative bias percentage of CA concentration for three simulated models (model 1, 2, and 3) in different relative bias of flip angle

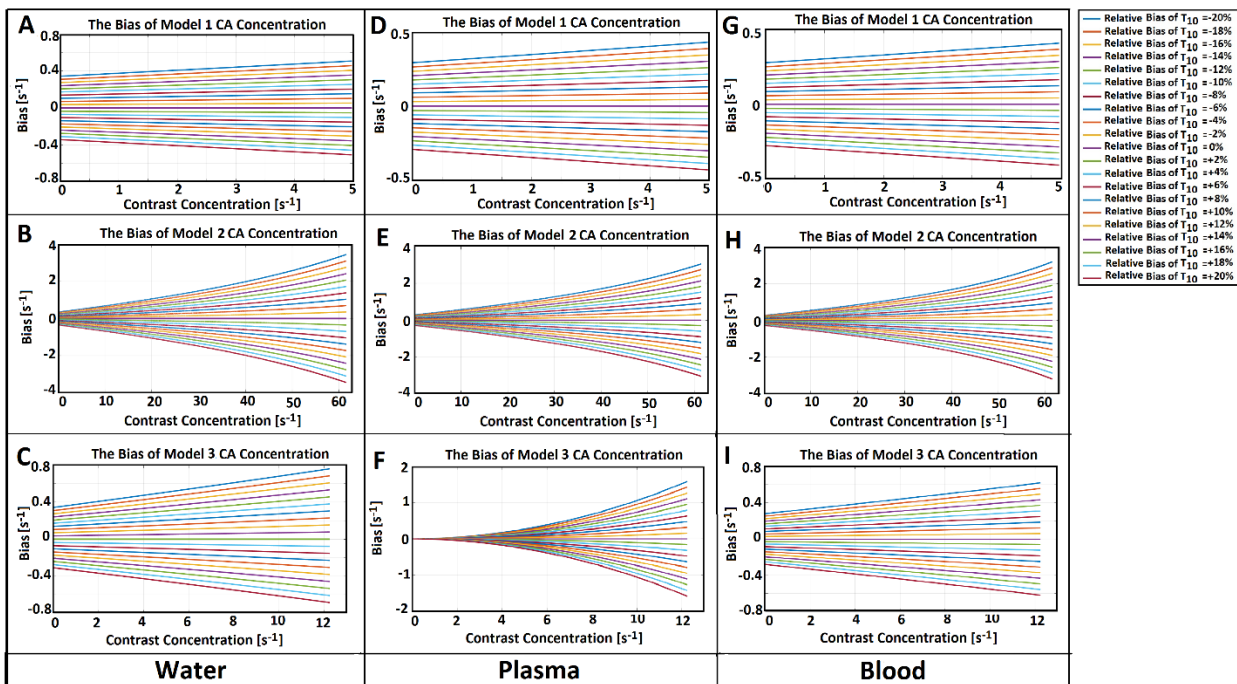


Figure 4. This figure illustrates the bias of the CA concentration of three simulated models, as compared to different concentration values at different relative bias of T_{10} . A) the bias of model 1 CA concentration in water part of the brain, B) the bias of model 2 CA concentration in water part of the brain, C) the bias of model 3 CA concentration in water part of the brain, D) the bias of model 1 CA concentration in plasma part of the brain, E) the bias of model 2 CA concentration in plasma part of the brain, F) the bias of model 3 CA concentration in plasma part of the brain, G) the bias of model 1 CA concentration in blood part of the brain, H) the bias of model 2 CA concentration in blood part of the brain, I) the bias of Model 3 CA concentration in blood part of the brain

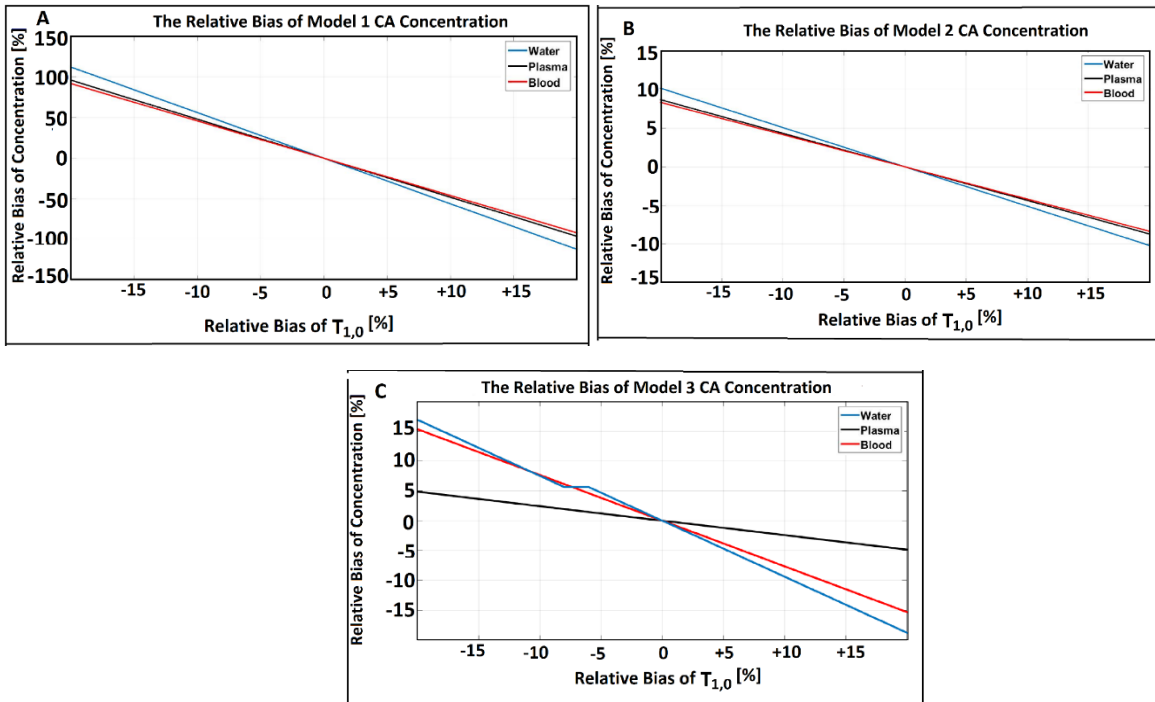


Figure 5. Mean relative bias percentage of CA concentration for three simulated models (Model 1, 2 and 3) in different relative bias of $T_{1,0}$

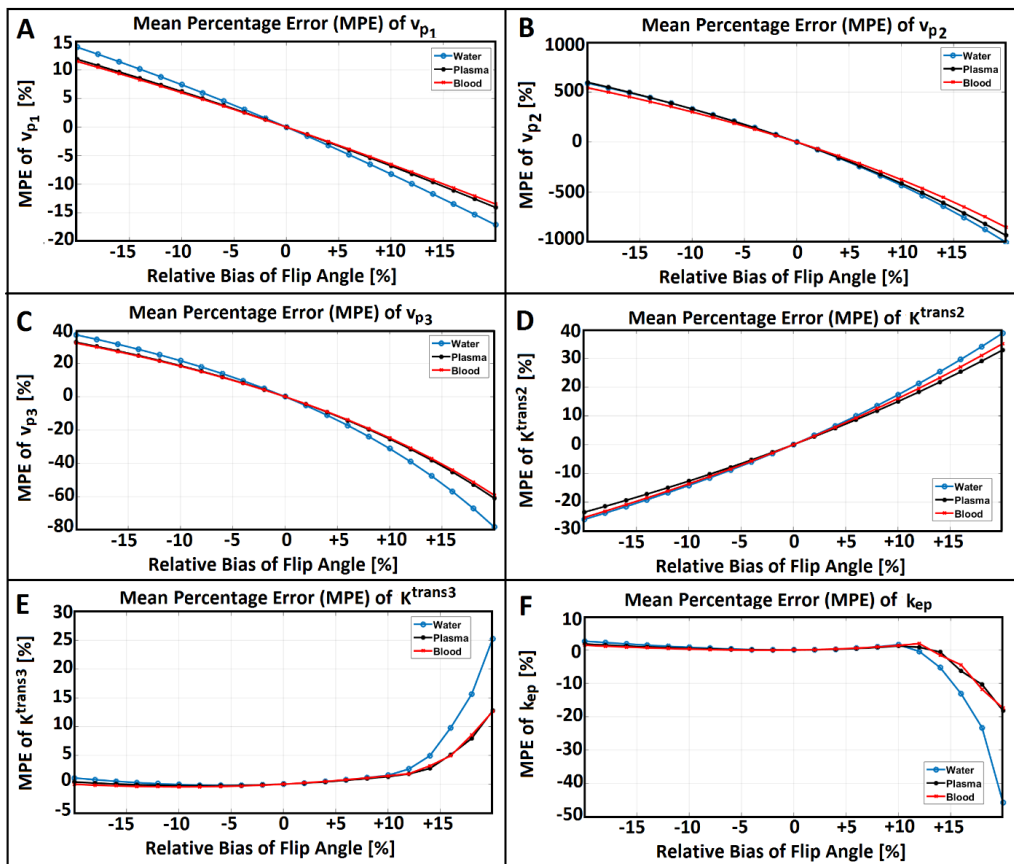


Figure 6. This figure depicts the Mean Percentage Error (MPE) of the estimated PK parameters in different relative bias of flip angle for three brain tissues (Water, Plasma and Blood)

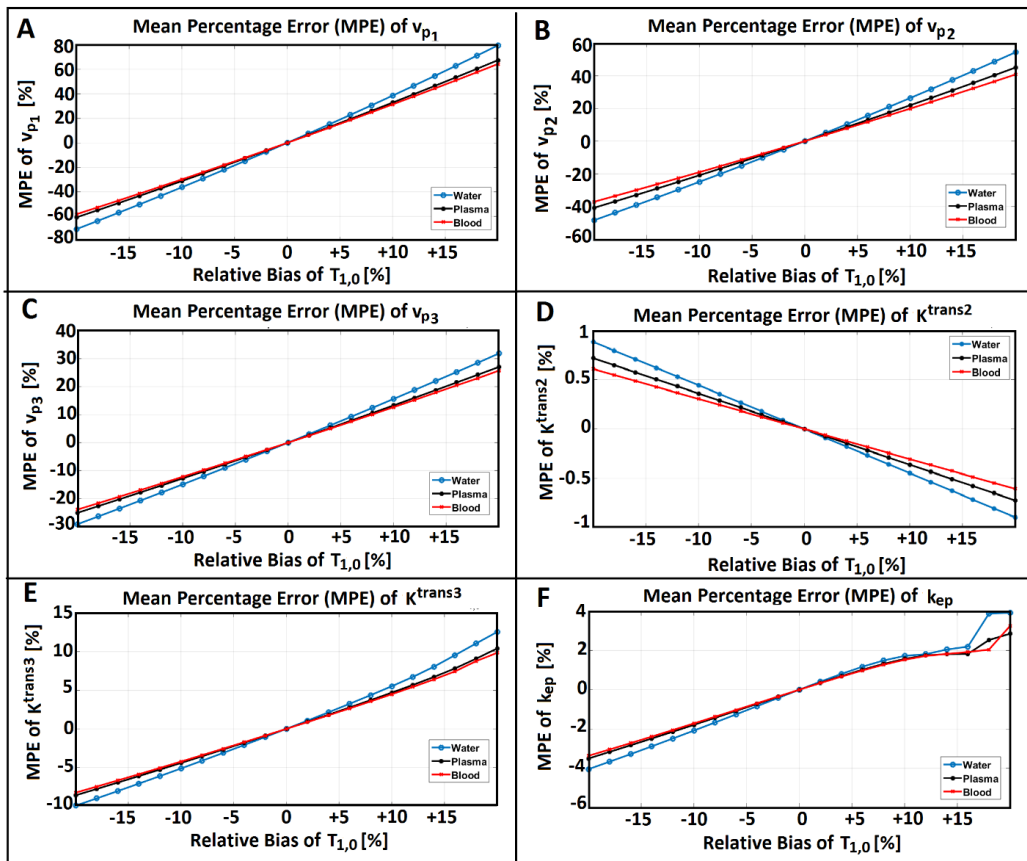


Figure 7. This figure shows the MPE of the estimated PK parameters in different relative bias of $T_{1,0}$ for three brain tissues (Water, Plasma and Blood)

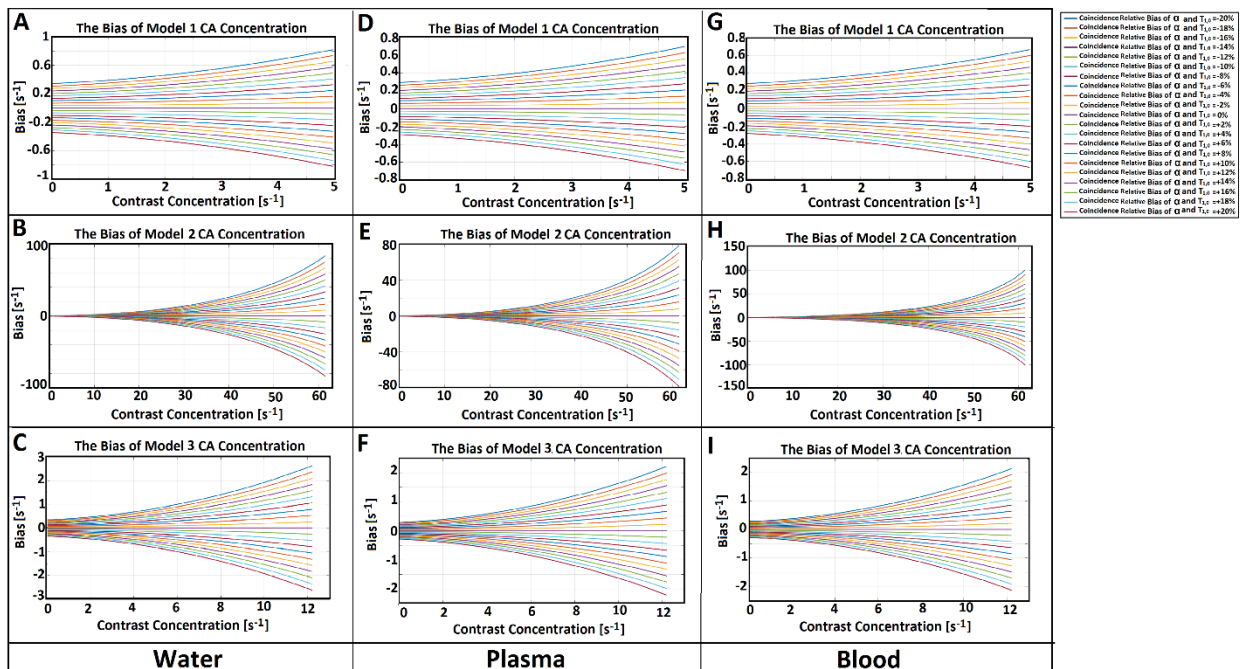


Figure 8. This figure illustrates the bias of the CA concentration of three simulated models contrary to different concentration values at different coincidence relative bias of flip angle and $T_{1,0}$. A) the bias of model 1 CA concentration in water part of the brain, B) the bias of model 2 CA concentration in water part of the brain, C) the bias of model 3 CA concentration in water part of the brain, D) the bias of model 1 CA concentration in plasma part of the brain, E) the bias of model 2 CA concentration in plasma part of the brain, F) the bias of model 3 CA concentration in plasma part of the brain, G) the bias of model 1 CA concentration in blood part of the brain, H) the bias of model 2 CA concentration in blood part of the brain, I) the bias of Model 3 CA concentration in blood part of the brain

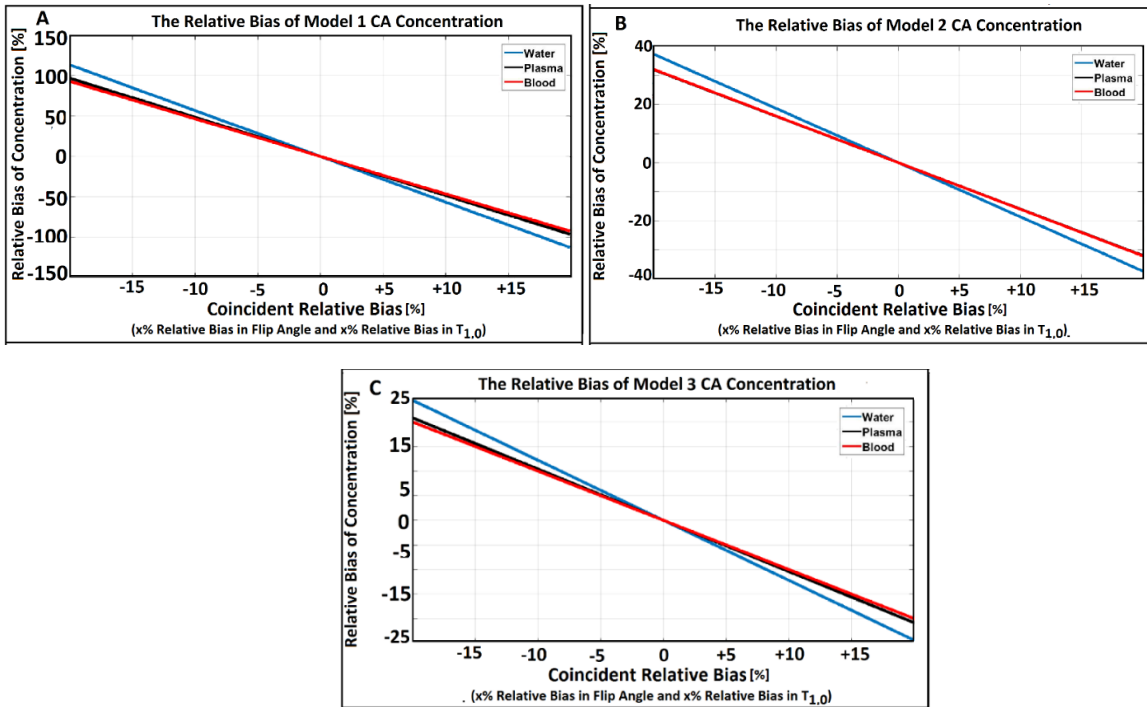


Figure 9. Mean relative bias percentage of CA concentration for three simulated models (Model 1, 2 and 3) in different coincidence relative bias of flip angle and $T_{1,0}$

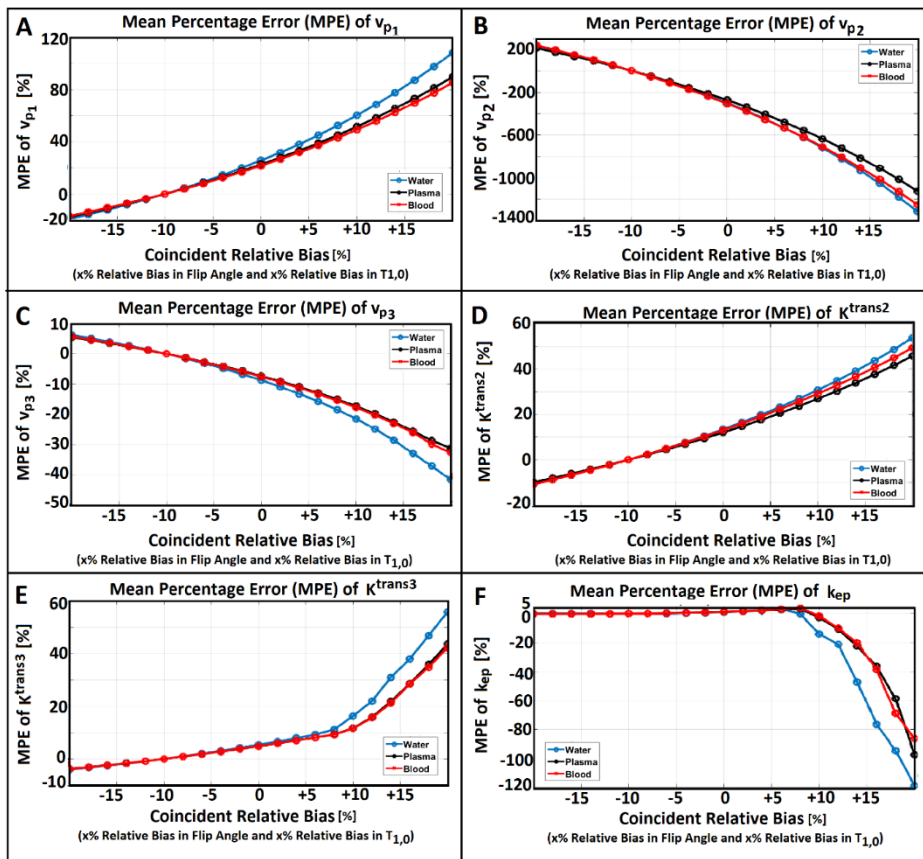


Figure 10. This figure demonstrates the MPE of the estimated PK parameters in different coincidence relative bias of flip angle and $T_{1,0}$ for three brain tissues (Water, Plasma and Blood)

Figure 5 illustrates the mean relative bias percentage of the CA concentration, in comparison to different relative biases of $T_{1,0}$. As depicted in Figure 5, the relative bias of concentration in water is higher (~1.5 to ~2 times), as compared to plasma and blood parts of the brain in all studied bias range of $T_{1,0}$. Figures 2-5 display that the effect of flip angle bias on the CA concentration uncertainty (except for Model 1) is more important than the effect of the same relative biases in $T_{1,0}$.

The mean percentage error (MPE) of each estimated PK parameter was computed for analyzing the precision of the pharmacokinetic parameters, when predicted from the biased CA concentration and AIF profiles. Figure 6 shows that blood plasma volume (v_p) is the most sensitive parameter to flip angle variations, especially v_p in Model 2 that may overestimate more than 800% in +20% relative bias in α . Forward transfer constant (K^{trans}) of Model 2 was found as another sensitive parameter to the bias of α , which may under or overestimate up to ~-25% and ~+40% in -20% and +20% relative bias of flip angle, respectively. The backward transfer constant (k_{ep}) and K^{trans} of Model 3 show very weak dependency on underestimation in flip angle, while for positive bias of flip angle, $K^{\text{trans}3}$ may overestimate up to 13% in plasma and blood or 25% in water and k_{ep} may overestimate up to 19% in blood and plasma, or 46% in water tissue. Figure 7 demonstrates that the most sensitive PK parameter to the bias of $T_{1,0}$ is v_p , especially v_p of Model 1 that may overestimate up to 80%. In addition, K^{trans} of Model 2 has lowest sensitivity to variation of $T_{1,0}$ and its MPE is less than $\pm 1\%$ in all investigated range of $T_{1,0}$ relative bias. A positive bias in $T_{1,0}$ causes overestimation in PK parameters, whereas a negative bias in $T_{1,0}$ leads to underestimation in PK parameters. However, K^{trans} of Model 2 demonstrates inverse behavior.

Furthermore, the effect of coincidence bias in flip angle and $T_{1,0}$ on the CA concentration bias was assessed since under or overestimation may simultaneously occur in flip angle and pre-contrast longitudinal relaxation time in real imaging conditions. The results of this evaluation is presented in Figures 8-10. Figure 9 clearly indicates that simultaneous incorporation of flip angle and $T_{1,0}$ bias may induce a large uncertainty in CA concentration profiles and consequently causes a significant bias in estimated PK parameters (Figure 10). As depicted in figure-10, the estimated PK parameters are more biased in water tissue, as compared to plasma or blood. Additionally, the overestimation in α and $T_{1,0}$ is revealed to make higher and more remarkable MPE in kinetic parameters. For instance, for 20% relative bias in each α and $T_{1,0}$, mean percentage error of computed parameters in three tissues are as following: MPE of v_{p1} is within the range of 80%-100%, MPE of v_{p2} is about 1100%-1300%, MPE of v_{p3} is around 30%-42%, MPE of $K^{\text{trans}2}$ is $> 45\%$

and $< 55\%$, MPE of $K^{\text{trans}3}$ is almost 40%-55%, and MPE of k_{ep} is within the range of 80%-120%.

Discussion

The tissue physiological parameters (including PK parameters) can provide valuable information regarding the tissue that can be applied in disease diagnosis and treatment process [1, 3, 4, 22-24]. In this respect, the accurate estimation of PK parameters derived from noninvasive imaging techniques, such as DCE-MRI is very beneficial to clinical diagnosis and treatment. To the best of our knowledge, a few studies investigated the effect of the bias in intrinsic tissue properties and imaging sequence parameters on the uncertainty of the time-CA concentration curves [8, 11, 12]. On the same note, little effort has been made to reduce these uncertainties by optimization of imaging acquisition process [6, 20, 25, 26]. Presumably, there exists no substantial study on the investigation and quantification of the effect of major sources of bias, such as inconsistency in flip angle (α) and pre-contrast longitudinal relaxation time ($T_{1,0}$) on the precision of the PK parameters considering the model selection concept.

The current study aimed at assessing the effect of bias in intrinsic properties of tissue, such as pre-contrast longitudinal relaxation time ($T_{1,0}$) and imaging sequence parameters, such as flip angle (α) on the error of estimated kinetic parameters in brain DCE-MRI studies. The obtained results clearly indicated that bias in α and $T_{1,0}$ generates uncertainty in measured CA concentration. Pharmacokinetic analysis of DCE-MRI studies is usually performed based on a pharmacokinetic model and the time-CA concentration signals; therefore, bias in time CA concentration profiles propagates to estimated PK parameters [7, 8, 11, 12]. The achieved results confirmed that Model 2 CA concentration uncertainty is more sensitive to flip angle bias, as compared to other two models, while Model 1 and 3 CA concentration uncertainty is more sensitive to $T_{1,0}$ bias and is not so sensitive to flip angle variation.

The relative bias in flip angle was reported to be usually about 3-10%, based on the studies which investigated the accurate measurement of flip angle and the difference between the real value from its nominal value [25, 26]. The error in fast measurement of $T_{1,0}$ was reported as 2-8%, depending on the measurement technique [20, 25, 27]. For this measured range of bias in DCE-MRI studies ($\sim \pm 10\%$ relative bias in α and $T_{1,0}$), the obtained results are as following: the maximum mean relative bias of Model 1 CA concentration in different brain tissues is 0.5% and 40-50% in effect of flip angle and $T_{1,0}$ bias, respectively. In addition, the maximum mean relative bias of Model 2 CA concentration, is about 10-12% and 4-5% in this range of relative bias of α and $T_{1,0}$ respectively. Furthermore, Figures 5 and 7 demonstrate the maximum percentage mean relative bias of Model 3 CA concentration as 3-4% and 2-10% for -10% to +10% relative bias in α and $T_{1,0}$, respectively.

Moreover, the results indicated that the major influence of $T_{1,0}$ and flip angle bias is on the blood plasma volume (v_p). In the reported range of bias in α (-10% to +10%), the mean percentage error (MPE) of v_{p1} was about 5-7% in blood and plasma; however, it was reported to be slightly higher in water section of the brain. The MPE of v_{p2} in this range of flip angle bias was about 400% in all three tissues; however, in blood part of the brain, the bias of this parameter was revealed to be a bit less, as compared to the two other tissues. MPE of v_{p3} is 20-30% in all three tissues, although it is higher in water, in comparison with blood and plasma. The behavior of the MPE for the plasma volumes in three models regarding $T_{1,0}$ bias is totally different from their relation to flip angle bias. An overestimation in $T_{1,0}$ leads to overestimation and an underestimation in $T_{1,0}$ produces underestimation in estimated plasma volumes. Furthermore, bias in $T_{1,0}$ generates a greater MPE of the v_{p1} s (~4 to 5 times), as compared to bias in flip angle, whereas MPE of v_{p2} affected by $T_{1,0}$ bias was much smaller (~1/12 times) than induced MPE by flip angle bias.

Among the forward and backward transfer constants in Model 2 and 3, just the MPE of the forward transfer constants in Model 2 in effect of flip angle bias was remarkable (~10%-15%), while MPE of the forward and backward transfer constants in Model 3 were negligible (<3%). In addition, the MPE of transfer constants in Model 2 and 3 in effect of $T_{1,0}$ bias were also insignificant for all three investigated tissues.

Presence the simultaneous bias in flip angle and $T_{1,0}$ on the CA concentration profiles additively bias the PK parameters. For example, for this bias range of α and $T_{1,0}$ (-10% to +10%), coincidence bias in these two parameters leads to overestimate up to 50% or underestimate up to 700% and 20% for the plasma volume in Model 1, 2 and 3, respectively. Forward transfer constant for Model 2 may overestimate up to 30%, whereas the mean variations of forward and backward transfer constants for Model 3 would be < 20%.

Conclusion

Based on the results of the current study, α and $T_{1,0}$ deviations were revealed to result in important errors in plasma volume estimation of brain tissues through Tofts-model fitting, while the estimation of transfer constants could be more reliable and robust in the presence of deviation in flip angle or pre-contrast longitudinal relaxation time in brain DCE-MRI studies. Although the major contributor to the transfer constants bias is flip angle overestimation, inconsistency in tuned flip angle may induce significant error on transfer constants parameters. In this evaluation, we used an identified imaging sequence parameters and Signal-to-noise ratio (SNR). The results can be dependent on these parameters; therefore, more investigations are needed to evaluate the dependency of the PK parameters on imaging sequence parameters, especially SNR of DCE-MR images.

Finally, it is worthy to note that utilization of a nested model selection technique, along with a robust and accurate estimator, such as MLE algorithm, created a unique approach of investigation for investigating the effect of propagation of the bias in the CA concentration measurement to the estimated PK parameters without adding extra biases to the parameters during the estimation, which was absent in most of the previous studies.

References

1. Aryal MP, Nagaraja TN, Keenan KA, Bagher-Ebadian H, Panda S, Brown SL, Cabral G, Fenstermacher JD, Ewing JR: Dynamic Contrast Enhanced MRI Parameters and Tumor Cellularity in a Rat Model of Cerebral Glioma at 7T. *Magn Reson in Med* 2014, 71:2206-2214.
2. Heye AK, Culling RD, Valdés Hernández MdC, Thrippleton MJ, Wardlaw JM: Assessment of blood-brain barrier disruption using dynamic contrast-enhanced MRI. A systematic review. *NeuroImage: Clinical* 2014, 6:262-274.
3. Mills SJ, du Plessis D, Pal P, Thompson G, Buonacorsi G, Soh C, Parker GJ, Jackson A: Mitotic Activity in Glioblastoma Correlates with Estimated Extravascular Extracellular Space Derived from Dynamic Contrast-Enhanced MR Imaging. *AJNR Am J Neuroradiol* 2015, 37:811-817.
4. Dehkordi ANV, Kamali-Asl A, Wen N, Mikkelsen T, Chetty IJ, Bagher-Ebadian H: DCE-MRI prediction of survival time for patients with glioblastoma multiforme: using an adaptive neuro-fuzzy-based model and nested model selection technique. *NMR Biomed* 2017, 30.
5. Bagher-Ebadian H, Jain R, Nejad-Davarani SP, Mikkelsen T, Lu M, Jiang Q, Scarpace L, Arbab AS, Narang J, Soltanian-Zadeh H, et al: Model selection for DCE-T1 studies in glioblastoma. *Magn Reson Med* 2012, 68:241-251.
6. Wang P, Xue Y, Zhao X, Yu J, Rosen M, Song HK: Effects of Flip Angle Uncertainty and Noise on the Accuracy of DCE-MRI Metrics: Comparison Between Standard Concentration-Based and Signal Difference Methods. *Magnetic resonance imaging* 2015, 33:166-173.
7. Giovanni PD, Azlan CA, Ahearn TS, Semple SI, Gilbert FJ, Redpath TW: The accuracy of pharmacokinetic parameter measurement in DCE-MRI of the breast at 3 T. *Physics in Medicine & Biology* 2010, 55:121.
8. Subashi E, Choudhury KR, Johnson GA: An analysis of the uncertainty and bias in DCE-MRI measurements using the spoiled gradient-recalled echo pulse sequence. *Med Phys* 2014, 41:032301.
9. Calamante F: Arterial input function in perfusion MRI: a comprehensive review. *Prog Nucl Magn Reson Spectrosc* 2013, 74:1-32.
10. Keil VC, Mädler B, Gieseke J, Fimmers R, Hattingen E, Schild HH, Hadizadeh DR: Effects of arterial input function selection on kinetic parameters in brain dynamic contrast-enhanced MRI. *Magnetic Resonance Imaging* 2017, 40:83-90.
11. Schabel MC, Parker DL: Uncertainty and bias in contrast concentration measurements using spoiled

- gradient echo pulse sequences. *Phys Med Biol* 2008, 53:2345-2373.
12. De Naeyer D, De Deene Y, Ceelen WP, Segers P, Verdonck P: Precision analysis of kinetic modelling estimates in dynamic contrast enhanced MRI. *Magnetic Resonance Materials in Physics, Biology and Medicine* 2011, 24:51-66.
 13. Kershaw LE, Buckley DL: Precision in measurements of perfusion and microvascular permeability with T1-weighted dynamic contrast-enhanced MRI. *Magn Reson Med* 2006, 56:986-992.
 14. Ewing JR, Bagher-Ebadian H: Model Selection in Measures of Vascular Parameters using Dynamic Contrast Enhanced MRI: Experimental and Clinical Applications. *NMR in biomedicine* 2013, 26:1028-1041.
 15. Bagher-Ebadian H, Dehkordi A, Ewing J: SU-F-I-26: Maximum Likelihood and Nested Model Selection Techniques for Pharmacokinetic Analysis of Dynamic Contrast Enhanced MRI in Patients with Glioblastoma Tumors. *Medical Physics* 2016, 43:3392-3392.
 16. Dehkordi ANV, Alireza KA, R. EJ, Ning W, J. CI, Hassan BE: An adaptive model for rapid and direct estimation of extravascular extracellular space in dynamic contrast enhanced MRI studies. *NMR in Biomedicine* 2017, 30:e3682.
 17. Tofts PS, Berkowitz B, Schnall MD: Quantitative analysis of dynamic Gd-DTPA enhancement in breast tumors using a permeability model. *Magn Reson Med* 1995, 33:564-568.
 18. Röhrer M, Bauer H, Mintorovitch J, Requardt M, Weinmann HJ: Comparison of magnetic properties of MRI contrast media solutions at different magnetic field strengths. *Invest Radiol* 2005, 40:715-724.
 19. Gelman N, Ewing JR, Gorell JM, Spickler EM, Solomon EG: Interregional variation of longitudinal relaxation rates in human brain at 3.0 T: relation to estimated iron and water contents. *Magn Reson Med* 2001, 45:71-79.
 20. Deichmann R: Fast high-resolution T1 mapping of the human brain. *Magn Reson Med* 2005, 54:20-27.
 21. Myung IJ: Tutorial on maximum likelihood estimation. *Journal of Mathematical Psychology* 2003, 47:90-100.
 22. Ewing JR, Knight RA, Nagaraja TN, Yee JS, Nagesh V, Whitton PA, Li L, Fenstermacher JD: Patlak plots of Gd-DTPA MRI data yield blood-brain transfer constants concordant with those of ¹⁴C-sucrose in areas of blood-brain opening. *Magnetic Resonance in Medicine* 2003, 50:283-292.
 23. Jia ZZ, Gu HM, Zhou XJ, Shi JL, Li MD, Zhou GF, Wu XH: The assessment of immature microvascular density in brain gliomas with dynamic contrast-enhanced magnetic resonance imaging. *Eur J Radiol* 2015, 84:1805-1809.
 24. Li X, Zhu Y, Kang H, Zhang Y, Liang H, Wang S, Zhang W: Glioma grading by microvascular permeability parameters derived from dynamic contrast-enhanced MRI and intratumoral susceptibility signal on susceptibility weighted imaging. *Cancer Imaging* 2015, 15:4.
 25. Treier R, Steingoetter A, Fried M, Schwizer W, Boesiger P: Optimized and combined T1 and B1 mapping technique for fast and accurate T1 quantification in contrast-enhanced abdominal MRI. *Magn Reson Med* 2007, 57:568-576.
 26. Yarnykh VL: Actual flip-angle imaging in the pulsed steady state: a method for rapid three-dimensional mapping of the transmitted radiofrequency field. *Magn Reson Med* 2007, 57:192-200.
 27. Deoni SC, Rutt BK, Peters TM: Rapid combined T1 and T2 mapping using gradient recalled acquisition in the steady state. *Magn Reson Med* 2003, 49:515-526.